

Aromatic and olefinic C–H alkenylation by catalysis with spirocyclic NHC Ru(IV) pincer complex

Heng Cai¹, Yong-Qiang Tu^{1,2*}, Ka Lu¹, Qi-Long Chen¹, Fu-Min Zhang¹, Xiao-Ming Zhang¹, Yuan-Jiang Pan³ & Zhi-Bo Yan¹

¹State Key Laboratory of Applied Organic Chemistry & College of Chemistry and Chemical Engineering, Lanzhou University, Lanzhou 730000, China;

²School of Chemistry and Chemical Engineering, Frontiers Science Center for Transformative Molecules, Shanghai Jiao Tong University, Shanghai 200240, China;

³Department of Chemistry, Zhejiang University, Hangzhou 310027, China

Received December 27, 2022; accepted February 9, 2023; published online April 10, 2023

Catalyst innovation lies at the heart of transition-metal-catalyzed reaction development. In this article, we have explored the C(sp²)-H alkenylation activity with novel spirocyclic N-heterocyclic carbene (NHC)-based cyclometalated ruthenium pincer catalyst system, **SNRu-X**. After screening catalyst and condition, a high valent Ru(IV) dioxide (X = O₂) species has demonstrated superior reactivity in the catalytic alkenylation of aromatic and olefinic C–H bonds with unactivated alkenyl bromides and triflates. This reaction has achieved the easy construction of a wide range of (hetero)aromatic alkenes and dienes, in good to excellent yields with exclusive selectivity. Preliminary mechanistic studies indicate that this reaction may proceed through a single electron transfer (SET) triggered oxidative addition, by doing so, providing valuable complementary to classical alkenylation reactions that are dependent on activated alkenyl precursors.

transitionmetal catalysis, spirocyclic NHC-Ru pincer catalyst, C–H alkenylation, single electron transfer pathway, unactivated alkenyl bromides and triflates

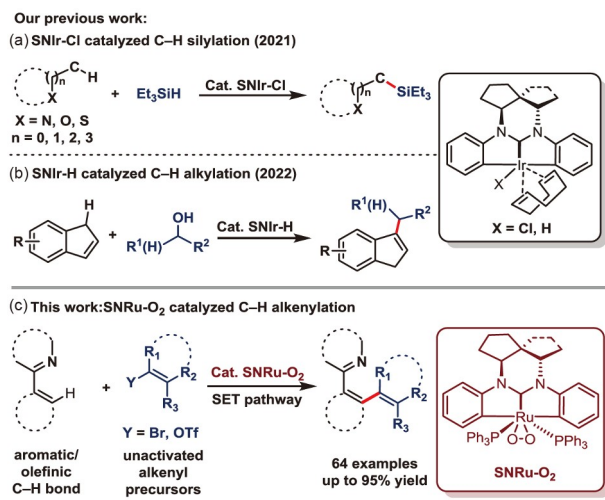
Citation: Cai H, Tu YQ, Lu K, Chen QL, Zhang FM, Zhang XM, Pan YJ, Yan ZB. Aromatic and olefinic C–H alkenylation by catalysis with spirocyclic NHC Ru(IV) pincer complex. *Sci China Chem*, 2023, 66: 2791–2796, <https://doi.org/10.1007/s11426-022-1541-5>

1 Introduction

Transition-metal-catalyzed C–H bond activation reactions have emerged as a powerful strategy to forge C–C bonds in organic synthesis. The rational design of transition-metal catalyst structures, in particular the outer ligand framework, has great potential to enhance the reactivity and expand substrate scope, or even create new reaction mode [1,2]. In 2014 our group designed and explored a novel N-heterocyclic carbene (NHC) that contains a flexible 6-membered-ring fused with a rigid spirobicycle [3]. Late in 2021, we reported its cyclometalated CCC Ir(III)-pincer complex

(**SNIr-CI**) that demonstrated high reactivity, regioselectivity (α , β , γ or σ -positions), and chemoselectivity (sp² or sp³ hybridized C–H bonds) in the heteroatom-directed silylation of C–H bonds (Scheme 1a) [4]. Recently, an Ir(III) complex hydride catalyst (**SNIr-H**) has been found to enable selective benzylic alkylations with alcohols as alkyl donors (Scheme 1b) [5]. Mechanistic studies indicate that both of the above processes feature the formation of a flexible and hemi-open catalytic intermediate that can accommodate and activate substrates of different sizes, thus enabling the transfer of active species during the reaction. Inspired by these successes, we postulate that incorporation of other transition-metals into this unique NHC framework could generate further novel catalytic systems that are expected to display

*Corresponding author (email: tuyq@lzu.edu.cn, tuyq@sjtu.edu.cn)



Scheme 1 Spirocyclic NHC-based metal catalyst-enabled C–H functionalizations (color online).

some more reactivities than ever. With this in mind, ruthenium (Ru) has been examined due to its relatively low-cost [6] and the significant success in its cyclometalated Ru-complexes' catalytic functionalizations of inert C–H bond [7,8].

(Hetero)aryl alkenes and dienes have been used widely as versatile industrial and laboratory chemicals in organic synthesis [9]. Recent studies in transition-metal-catalyzed C–H bond functionalizations have generated some straightforward approaches to access these valuable π -conjugated molecules. For example, the manipulation of aromatic C–H bonds for the addition of alkyne fragments [10], or oxidative coupling with alkene partners [11]. Despite these advances, the existing methods have inherent limitations such as difficulty in synthesizing sterically hindered tetra-substituted alkenes, or the requirement of stoichiometric quantities of oxidant. To address these challenges, transition-metal-catalyzed aromatic C–H bond alkenylations with alkenyl (pseudo)halides have been developed [12] that can selectively access a structure diversity of products under redox-neutral conditions. However, such an alkenylation approach is heavily dependent upon the use of activated alkenyl halides such as bromostyrenes and bromoacrylates, whereas unactivated alkenyl precursors still display significantly lower reactivity [13]. In addition, all aforementioned catalytic strategies are challenging to be extended to alkenylation of olefinic C–H bond due to the following difficulties: (1) olefinic C–H bond metalations are much harder than those of arenes; (2) unwanted conjugate addition, oxidation or polymerization of the olefinic π -bond are easy to take place. Indeed, for example, there is only one isolated report on olefinic C–H bond coupling with alkenyl halides (using 5 equivalents of CF₃- or C₂F₅-substituted/activated alkenyl bromide) [13d]. Consequently, design and development of an

alternative catalytic system that is capable of realizing both aromatic and olefinic C–H alkenylations, and more importantly compatible with unactivated alkene precursors, would be of significant demand for organic synthesis, but still remain challenging. Herein, we report our research efforts toward this goal by developing a novel class of cyclometalated Ru pincer catalysts, such as **SNRu-O₂** (Scheme 1c), that incorporate a unique spirocyclic NHC framework mentioned above [3–5]. This reaction offers a valuable alternative to some classic alkenylation reactions that generally use the activated alkenyl coupling partners, such as the Nobel Prize winning Heck reaction.

2 Results and discussion

We began our studies with the synthesis of several spirocyclic NHC-based Ru pincer complexes, **Cat. A**, **B** and **C**, where Ru possesses the IV, III and II oxidation states, respectively (Table 1). Pleasingly, these complexes could be easily accessed and all bench stable (see the Supporting Information online for details). Remarkably, **Cat. A** contained an unusual Ru(IV)-dioxo motif. With these catalysts in hand, we chose 2-(*o*-tolyl)pyridine (**1a**) as a model substrate for the C–H alkenylation because it was prevalent in both medicinal and material research fields [9a,9d], and pyridine moiety or its analogues were also the commonly useful di-

Table 1 Catalyst screen and optimization of the reaction conditions^{a)}

Entry	Cat.	Solvent	<i>T</i> (°C)	Yield (%) ^{b)}
1	A	THF	120	84
2	B	THF	120	78
3	C	THF	120	0
4	[RuCl ₂ (<i>p</i> -cymene)] ₂	THF	120	13
5	Cp(PPh ₃) ₂ RuCl	THF	120	0
6	RuCl ₃	THF	120	0
7	SNIr-Cl	THF	120	0
8	SNIr-H	THF	120	0
9	None	THF	120	0
10	A	1,4-dioxane	120	89
11	A	toluene	120	60
12 ^{c)}	A	1,4-dioxane	140	95

^{a)} General conditions: **1a** (0.2 mmol), **2a** (0.4 mmol), Cat. (5 mol%), K₂CO₃ (0.4 mmol) and solvent (0.5 mL) for 24 h under argon. ^{b)} Yields determined by ¹H NMR. ^{c)} 1,4-Dioxane (0.3 mL).

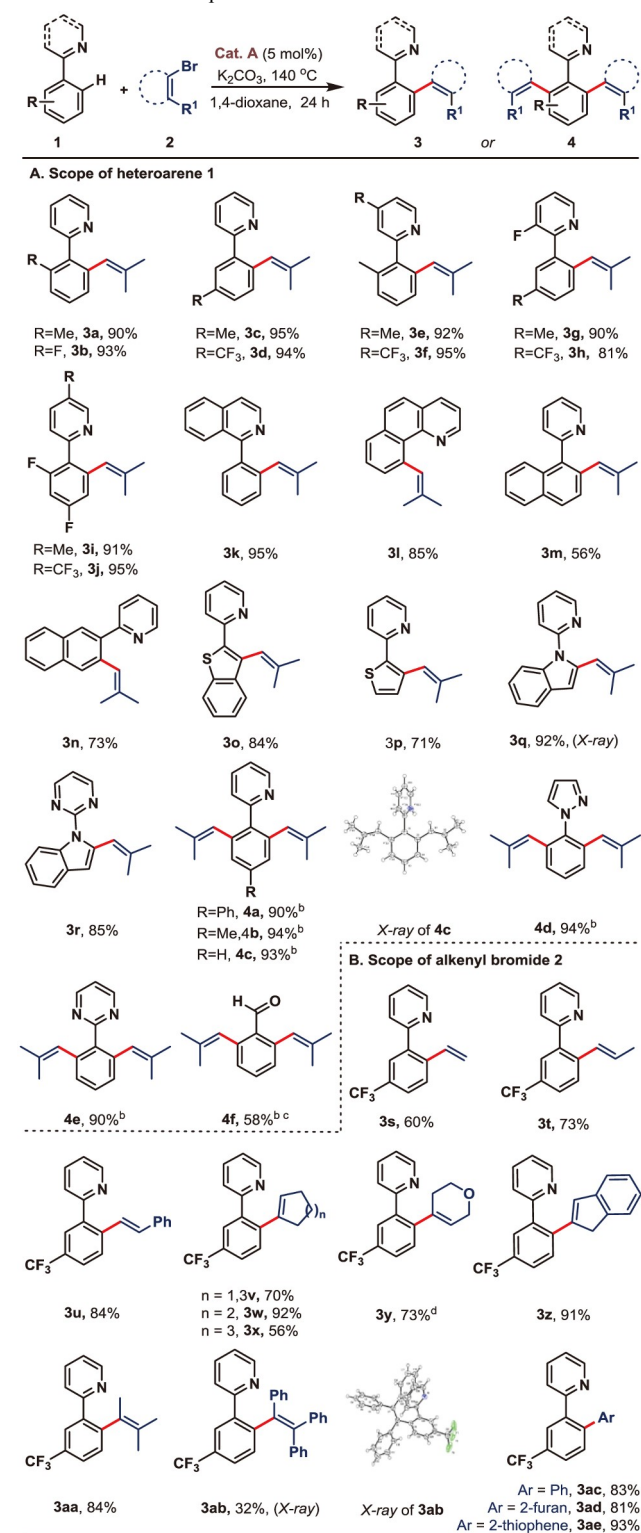
recting groups. An unactivated alkenyl bromide, 1-bromo-2-methylpropene (**2a**), was employed as a model alkenylation partner. Following extensive screening of reaction conditions and catalysts, we obtained the desired C–H alkenylation product **3a** in 84% yield using **Cat. A** (5 mol%), whereas **Cat. B** was less efficient and **Cat. C** failed to react (entries 1 vs. 2, 3). Some other commonly used Ru-catalysts were also examined, but all delivered a lower yield of **3a**, or behaved low or on reactivity (entries 4–6). When the previously mentioned Ir(III) catalysts (**SNIr-Cl** and **H**, entries 7, 8) were subjected to these conditions, no reaction was observed. A control experiment in the absence of the Ru-catalyst led to no product formation (entry 9). We then investigated different solvents (entries 10, 11), and 1,4-dioxane was found the most effective. Finally, an optimal 95% yield of **3a** was obtained by raising the reaction temperature to 140 °C, and the system concentration to 0.67 M (entry 12).

With optimized conditions in hand, the scope of the (hetero)arene substrate was first investigated and the results were shown in Table 2A. Substrates containing either EDGs or EWGs at the *o*- or *m*-position of the arene fragment (**3a–3j**) or fused benzene ring (**3k–3n**) reacted smoothly to give mono-alkenylation products in good to excellent yield (73%–95%). Exceptionally, a biphenyl containing substrate **3m** gave only the moderate yield (56%). Heteroaromatic substrates (**3o–3r**) also performed well, yielding the expected products in good to high yields. In most cases of Table 2A, the electronic effect of the substituents at substrates had a negligible effect on the reaction efficiency.

Subsequently, we tested the bis-alkenylation reaction (**4a–4f**). Wherever substrates exposed two active sites, reactions could generate the di-alkenylation products in excellent yields (>90%), although DG was employed (**4a–4e**). It was particularly noteworthy that a phenyl imine-directed reaction, followed by deamination, could give a final benzaldehyde product **4f** in good yield. Such a product bearing three adjacent substituents at one benzene ring was difficult to be obtained in a typical manner and would find good application.

Next, we examined the scope of the alkenyl bromide partner bearing up to three substituents, with 2-(*m*-trifluoromethyl phenyl)pyridine **1d** being the model substrate. Bromoethenes with various substituents can effectively generate heavily substituted aryl alkenes (Table 2B). And both *Z*- and *E*-1,2-disubstituted bromoethenes formed exclusively the *E*-product (**3t**, **3u**). Unactivated bromoalkenes, such as simple bromoethene (**3s**) and cyclic alkenyl bromides (**3v–3z**) were also well tolerated, with the cyclohexenyl (**3w**) and indenyl (**3z**) products being formed in excellent yields. Importantly, reactions with trisubstituted bromoalkenes **2** also performed well, producing the challenging olefins **3aa** and **3ab** with a crowded tetra-substitution, whose analogs were useful in optical and electronic

Table 2 Reaction scope^{a)}



a) Unless otherwise specified, reactions with **1** (0.2 mmol), **2** (0.4 mmol), **Cat. A** (5 mol%) and K₂CO₃ (0.4 mmol) in 1,4-dioxane (0.3 mL) at 140 °C under argon for 24 h, isolated yield. b) **2** (0.6 mmol). c) Substrate bearing a phenyl imine-DG used. d) **Cat. A** (10 mol%).

material sciences [14]. In addition, the (hetero)aromatic bromides **2** were typically workable toward this catalytic

system, affording the C–H arylated products **3ac–3ae** in good to excellent yields.

We then turned to expand the reactivity of our catalytic system to olefinic C–H alkenylations. This transformation was more challenging than that of arenes, as olefins tethered to pyridine were easy to undergo side-reactions in the presence of transition-metal catalysts and alkenyl halide electrophiles [15]. To our delight, when **2a** was used, a wide range of (*E*)-2-olefinpyridines could react smoothly to give exclusively the desired γ -alkenylation products under the standard condition (**6a–6r**, Table 3). Various γ -substituted substrates with primary (**5a–5d**), or secondary alkyls (**5e**, **5f**), or even sterically hindered aryls and heteroaryls (**5g–5p**), were also well tolerated, generating the corresponding products in moderate to good yields. In addition, alkenylation of cyclic olefins (**5q**, **5r**) performed well, giving sterically hindered tetrasubstituted olefin products (**6q**, **6r**) in good yield. To the best of our knowledge, the results in Table 3 were the first succeeded examples for olefinic C–H alkenylation using unactivated alkenyl precursors.

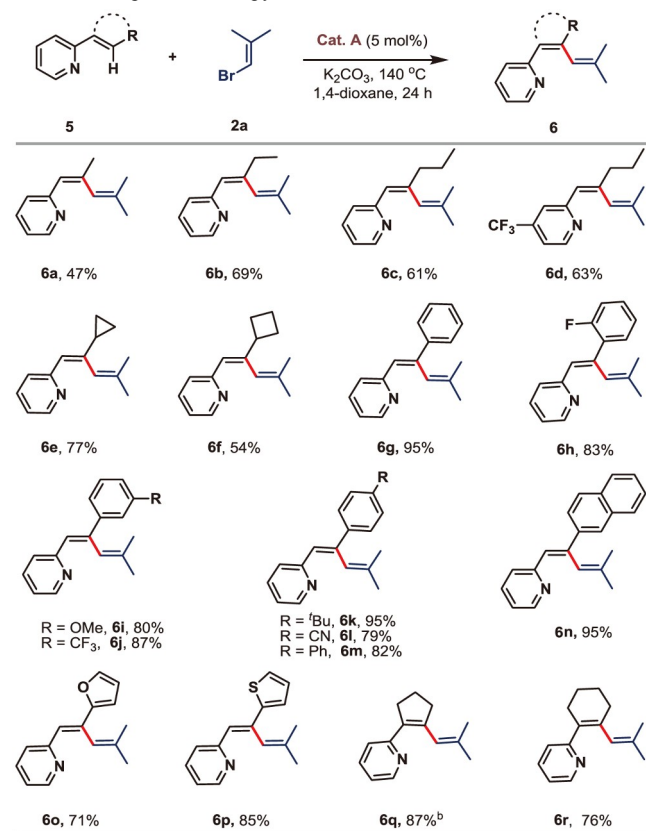
In addition, our investigation was turned to alternate the alkenyl bromide partners **2** with triflates **7**. Compared with the alkenyl bromides used above, alkenyl triflates were usually less utilized in alkenylations. However, the latter

could be easier to prepare from ketones or aldehydes, and thus would have wider utility if an active enough catalyst was available.

In view of this, a series of unactivated alkenyl triflates were subjected to examination of the reactivity of **Cat. A**. As indicated in Table 4, both cyclic and acyclic alkenyl triflates bearing neither activating nor stabilizing functionalities could react with 2-(*m*-trifluoromethyl phenyl) or 2-cyclopentenyl pyridines under the standard conditions. Remarkably, the aromatic C–H alkenylation proceeded with high efficiency, generating tri-substituted alkene products (**8a–8f**) in moderate to good yields, whereas the olefinic C–H alkenylation of cyclopentenyl pyridine delivered relatively lower yields of the diene products (**8g–8i**). These results clearly indicated **Cat. A** exhibited considerable reactivity towards unactivated alkenyl triflates, and further improvements of our catalyst SNRu-X will be of great potential utility.

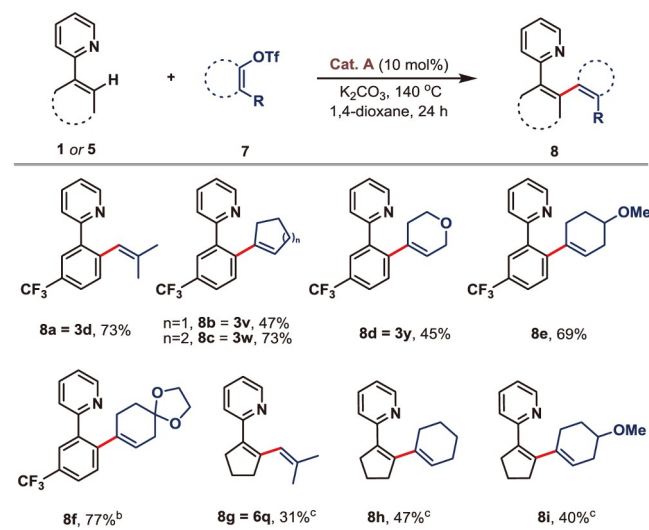
Several final experiments were conducted to obtain insights into the reaction mechanism (Scheme 2). Initially, a stoichiometric reaction of **Cat. A** and alkenyl bromide **2a** was performed at 50 °C (Scheme 2a), forming a Ru(III)-bromide species (**Cat. D**, confirmed by X-ray analysis) in 15% yield (0.0075 mmol). A complicated mixture of other components was not isolable and detectable. When **Cat. D** was used as a catalyst (5 mol%), **3a** was obtained in 85% yield (Scheme 2b), a result very similar to that obtained with **Cat. A** and **Cat. B** (Table 1). Furthermore, when TEMPO was used as a radical scavenger, the reaction afforded only a trace amount of **3a** (Scheme 2c). Taken altogether, these results suggested that all **Cat. A**, **B** and **D** were possibly the pre-catalysts that may generate the same Ru(II) species **I** (Figure 1 below) in the reaction that undergoes radical type

Table 3 Scope of 2-olefinpyridine substrates **5**^{a)}

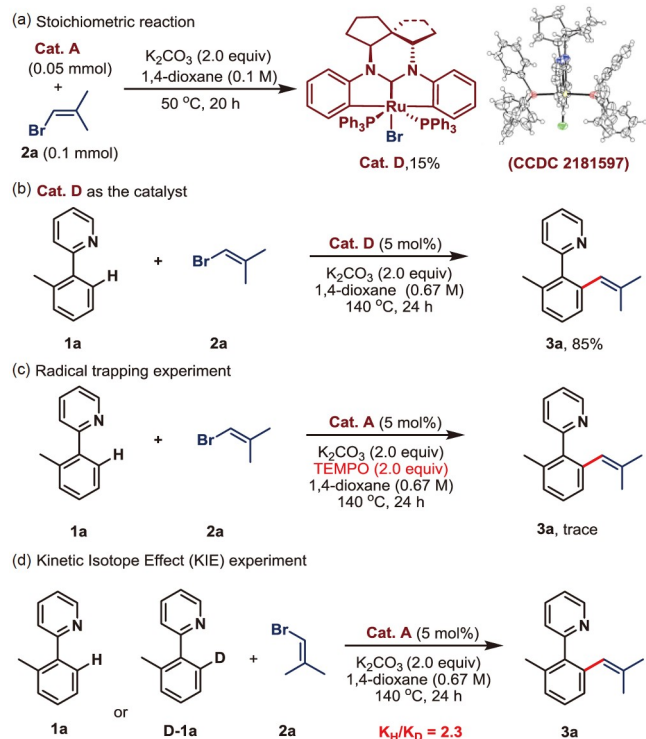


a) Unless otherwise specified, reactions with **5** (0.2 mmol), **2a** (0.4 mmol), **Cat. A** (5 mol%), and K₂CO₃ (0.4 mmol) in 1,4-dioxane (0.3 mL) at 140 °C under argon for 24 h, isolated yield. b) 48 h.

Table 4 Scope of the alkenyl triflates^{a)}



a) Unless otherwise specified, reactions with **1 or 5** (0.2 mmol), **7** (0.4 mmol), **Cat. A** (10 mol%), and K₂CO₃ (0.4 mmol) in 1,4-dioxane (0.3 mL) at 140 °C under argon for 24 h, isolated yield, b) 160 °C. c) **Cat. B** (10 mol%).



Scheme 2 Mechanistic experiments (color online).

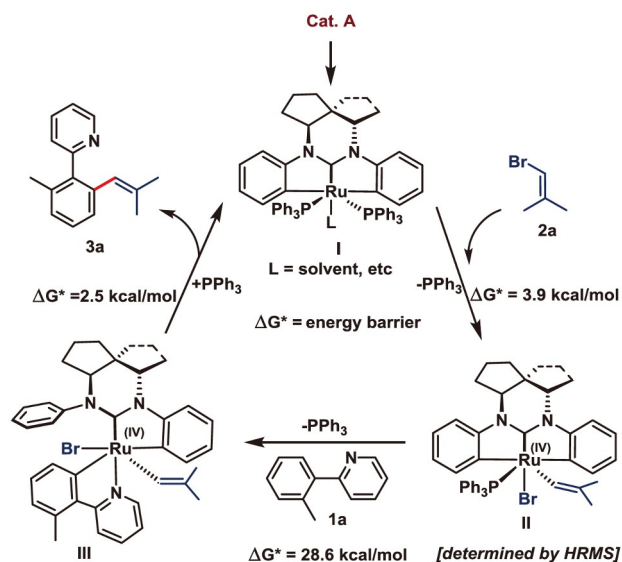


Figure 1 Proposed reaction mechanism (color online).

oxidative addition with the corresponding alkenyl bromide. Although an attempt to isolate and identify this on-cycle Ru (II) species **I** failed, several further observations were consistent with above conjecture: (1), the Ru species (species **II**, Figure 1, *vide infra*) generated by the oxidative addition step was detected by the real-time high resolution mass spectroscopy (HRMS) of the model reaction system (see the Supporting Information online for details); (2) the density functional theory (DFT) calculations indicated that the oxi-

dativ addition triggered by single electron transfer (SET) from Ru(II) species to alkenyl bromide (energy barrier $\Delta G^* = 3.9$ kcal/mol) was more feasible than concerted two-electron oxidative addition pathway ($\Delta G^* = 21.5$ kcal/mol) (see the Supporting Information online for details). The latter was unusual as unactivated alkenyl halides have a highly negative reduction potential, meaning that an SET-based generation of the highly unstable alkenyl radical would be a challenging process [16]. Finally, a kinetic isotope effect (KIE) experiment revealed a primary KIE of 2.3, suggesting that C–H cleavage would be the turnover limiting step (Scheme 2d) [17]. This was consistent with a competition experiment fact that revealed a significant reaction rate difference between *m*-EWG's phenyl substitution and the *m*-EDG's one (see the Supporting Information online for details).

Based on the acquired evidence and our previous understanding on the catalytic behavior of SNM-X [4,5], a tentative mechanism is proposed (Figure 1). **Cat. A** first *in situ* generate a Ru(II) species **I**, which subsequently undergoes radical type oxidative addition with alkenyl bromide **2a** to deliver a Ru(IV) species **II** (detected by real-time HRMS). Then, C–H ruthenation of **1a** by species **II** occurs, likely via a σ -bond metathesis pathway, generating a Ru(IV) species **III**, and this goes through reductive elimination to produce the final product **3a** and to complete the catalytic cycle. DFT calculations further supported our proposal that C–H activation of **1a** was the turnover limiting step with an energy barrier of 28.6 kcal/mol (**II** to **III**), whereas reductive elimination was exergonic ($\Delta G = -21.0$ kcal/mol) with a barrier of 2.5 kcal/mol (see the Supporting Information online for details). We speculated that the above particular catalytic activity **Cat. A** emerged would be attributed mainly to the strong carbenic complexing and σ -electron donating abilities of our spirocyclic 6-membered-ring's NHC ligand [3,18], the bulky stereo-hindrance of the complex molecular backbone as well as the special property of the central ruthenium.

3 Conclusions

In summary, we have developed a novel spirocyclic NHC-based cyclometalated Ru(IV) pincer catalyst, **Cat. A**, that contains a high valent and sterically crowded Ru dioxide center. Owing to its highly catalytic activity, we have realized the C–H alkenylation of both aromatic and olefinic substrates using unactivated alkenyl bromide and triflate partners. A wide range of multi-substituted (hetero)aryl alkenes and dienes were produced efficiently, indicating the potential utility of this reaction in synthetic chemistry. Preliminary mechanistic studies indicate that the reaction proceeds through a radical pathway. This alkenylation further displays the versatile reactivity of our SNM-X catalyst ser-

ies. Further investigations into this series are ongoing in our group.

Acknowledgements This work was supported by the National Natural Science Foundation of China (2187,1117, 91956203), the “111” Program of Minister of Education, Beijing National Laboratory for Molecular Sciences (BNLMS202109) and the Science and Technology Commission of Shanghai Municipality (19JC1430100). We also thank Prof. Lu Zhan (Zhejiang University) for his kind assistant HRMS analysis.

Conflict of interest The authors declare no conflict of interest.

Supporting information The supporting information is available online at chem.scichina.com and link.springer.com/journal/11426. The supporting materials are published as submitted, without typesetting or editing. The responsibility for scientific accuracy and content remains entirely with the authors.

- (a) Elsby MR, Baker RT. *Chem Soc Rev*, 2020, 49: 8933–8987; (b) Ibáñez S, Poyatos M, Peris E. *Acc Chem Res*, 2020, 53: 1401–1413; (c) Rogge T, Kaplaneris N, Chatani N, Kim J, Chang S, Punji B, Schafer LL, Musaev DG, Wencel-Delord J, Roberts CA, Sarpong R, Wilson ZE, Brimble MA, Johansson MJ, Ackermann L. *Nat Rev Methods Primers*, 2021, 1: 43; (d) Ott JC, Bürgy D, Guan H, Gade LH. *Acc Chem Res*, 2022, 55: 857–868; (e) Marciniak B, Pietraszuk C, Pawluć P, Maciejewski H. *Chem Rev*, 2022, 122: 3996–4090
- (a) Hartwig JF. *Acc Chem Res*, 2012, 45: 864–873; (b) Guisado-Barrios G, Soleilhavoup M, Bertrand G. *Acc Chem Res*, 2018, 51: 3236–3244; (c) Soleilhavoup M, Bertrand G. *Chem*, 2020, 6: 1275–1282; (d) Jazzar R, Soleilhavoup M, Bertrand G. *Chem Rev*, 2020, 120: 4141–4168; (e) Yazdani S, Junor GP, Peltier JL, Gembicky M, Jazzar R, Grotjahn DB, Bertrand G. *ACS Catal*, 2020, 10: 5190–5201; (f) Gao Y, Kim N, Mendoza SD, Yazdani S, Faria Vieira A, Liu M, Kendrick Iv A, Grotjahn DB, Bertrand G, Jazzar R, Engle KM. *ACS Catal*, 2022, 12: 7243–7247; (g) Wang Y, Huang Z, Liu G, Huang Z. *Acc Chem Res*, 2022, 55: 2148–2161
- Yang BM, Xiang K, Tu YQ, Zhang SH, Yang DT, Wang SH, Zhang FM. *Chem Commun*, 2014, 50: 7163–7165
- Yan ZB, Peng M, Chen QL, Lu K, Tu YQ, Dai KL, Zhang FM, Zhang XM. *Chem Sci*, 2021, 12: 9748–9753
- Dai K, Chen Q, Xie W, Lu K, Yan Z, Peng M, Li C, Tu Y, Ding T. *Angew Chem Int Ed*, 2022, 61: e202206446
- Palladium, Iridium, Rhodium and Ruthenium, Monthly Average Prices between 1st December 2017 and 1st December 2022. Johnson Matthey Precious Metals Management Home Page. <http://www.platinum.matthey.com/prices/price-charts> (accessed on 2022-12-15)
- (a) Arockiam PB, Bruneau C, Dixneuf PH. *Chem Rev*, 2012, 112: 5879–5918; (b) Leitch JA, Frost CG. *Chem Soc Rev*, 2017, 46: 7145–7153; (c) Nareddy P, Jordan F, Szostak M. *ACS Catal*, 2017, 7: 5721–5745; (d) Korvorapun K, Samanta RC, Rogge T, Ackermann L. *Synthesis*, 2021, 53: 2911–2946; (e) Findlay MT, Domingo-Legarda P, McArthur G, Yen A, Larrosa I. *Chem Sci*, 2022, 13: 3335–3362
- (a) Ackermann L. *Org Lett*, 2005, 7: 3123–3125; (b) Ackermann L, Born R, Álvarez-Bercedo P. *Angew Chem Int Ed*, 2007, 46: 6364–6367; (c) Ackermann L, Vicente R, Potukuchi HK, Pirovano V. *Org Lett*, 2010, 12: 5032–5035; (d) Kakiuchi F, Kochi T, Mizushima E, Murai S. *J Am Chem Soc*, 2010, 132: 17741–17750; (e) Saidi O, Marafie J, Ledger AEW, Liu PM, Mahon MF, Kociok-Köhn G, Whittlesey MK, Frost CG. *J Am Chem Soc*, 2011, 133: 19298–19301; (f) Hofmann N, Ackermann L. *J Am Chem Soc*, 2013, 135: 5877–5884; (g) Juliá-Hernández F, Simonetti M, Larrosa I. *Angew Chem Int Ed*, 2013, 52: 11458–11460; (h) Simonetti M, Perry GJP, Cambeiro XC, Juliá-Hernández F, Arokianathar JN, Larrosa I. *J Am Chem Soc*, 2016, 138: 3596–3606; (i) Simonetti M, Cannas DM, Just-Baringo X, Vitorica-Yrezabal IJ, Larrosa I. *Nat Chem*, 2018, 10: 724–731; (j) Simonetti M, Kuniyil R, Macgregor SA, Larrosa I. *J Am Chem Soc*, 2018, 140: 11836–11847; (k) Wang GW, Wheatley M, Simonetti M, Cannas DM, Larrosa I. *Chem*, 2020, 6: 1459–1468; (l) Korvorapun K, Kuniyil R, Ackermann L. *ACS Catal*, 2020, 10: 435–440; (m) Korvorapun K, Struwe J, Kuniyil R, Zangarelli A, Casnati A, Watterschoot M, Ackermann L. *Angew Chem Int Ed*, 2020, 59: 18103–18109; (n) Spencer ARA, Korde R, Font M, Larrosa I. *Chem Sci*, 2020, 11: 4204–4208; (o) Sagadevan A, Charitou A, Wang F, Ivanova M, Vuagnat M, Greaney MF. *Chem Sci*, 2020, 11: 4439–4443; (p) Wheatley M, Findlay MT, López-Rodríguez R, Cannas DM, Simonetti M, Larrosa I. *Chem Catal*, 2021, 1: 691–703
- (a) Liu KKC, Li J, Sakya S. *MRLC*, 2004, 4: 1105–1125; (b) Negishi E, Huang Z, Wang G, Mohan S, Wang C, Hattori H. *Acc Chem Res*, 2008, 41: 1474–1485; (c) Negishi E. *Angew Chem Int Ed*, 2011, 50: 6738–6764; (d) Mei J, Leung NLC, Kwok RTK, Lam JWY, Tang BZ. *Chem Rev*, 2015, 115: 11718–11940
- (a) Schipper DJ, Hutchinson M, Fagnou K. *J Am Chem Soc*, 2010, 132: 6910–6911; (b) Gao K, Lee PS, Fujita T, Yoshikai N. *J Am Chem Soc*, 2010, 132: 12249–12251; (c) Zhou B, Chen H, Wang C. *J Am Chem Soc*, 2013, 135: 1264–1267; (d) Halbritter G, Knoch F, Wolski A, Kisch H. *Angew Chem Int Ed Engl*, 1994, 33: 1603–1605
- (a) Arockiam PB, Fischmeister C, Bruneau C, Dixneuf PH. *Green Chem*, 2011, 13: 3075–3078; (b) Wang C, Chen H, Wang Z, Chen J, Huang Y. *Angew Chem Int Ed*, 2012, 51: 7242–7245; (c) Zhang H, Yang Z, Liu J, Yu X, Wang Q, Wu Y. *Org Chem Front*, 2019, 6: 967–971; (d) Zhang J, Lu X, Shen C, Xu L, Ding L, Zhong G. *Chem Soc Rev*, 2021, 50: 3263–3314
- (a) Matsuura Y, Tamura M, Kochi T, Sato M, Chatani N, Kakiuchi F. *J Am Chem Soc*, 2007, 129: 9858–9859; (b) Ye W, Luo N, Yu Z. *Organometallics*, 2010, 29: 1049–1052; (c) Ogiwara Y, Tamura M, Kochi T, Matsuura Y, Chatani N, Kakiuchi F. *Organometallics*, 2014, 33: 402–420; (d) Otley KD, Ellman JA. *Org Lett*, 2015, 17: 1332–1335; (e) Prakash S, Muralirajan K, Cheng CH. *Chem Commun*, 2015, 51: 13362–13364; (f) Zhao H, Xu X, Luo Z, Cao L, Li B, Li H, Xu L, Fan Q, Walsh PJ. *Chem Sci*, 2019, 10: 10089–10096; (g) Jiang X, Zeng Z, Hua Y, Xu B, Shen Y, Xiong J, Qiu H, Wu Y, Hu T, Zhang Y. *J Am Chem Soc*, 2020, 142: 15585–15594
- Herein, we refer styrene halides (possessing a conjugated (system) and acrylates halides (possessing an electron withdrawing activating group) as the activated alkenyl halides, and alkenyl halides without these activating factors, for example alkyl substituted electron neutral alkenyl halides, as unactivated alkenyl halides. Indeed, they showed significant lower reactivity in C–H bond alkenylation, see: (a) Gottmukkala AL, Derridj F, Djebbar S, Doucet H. *Tetrahedron Lett*, 2008, 49: 2926–2930; (b) Schneider C, Masi D, Couve-Bonnaire S, Pannecoucke X, Hoarau C. *Angew Chem Int Ed*, 2013, 52: 3246–3249; (c) Zhang W, Tian Y, Zhao N, Wang Y, Li J, Wang Z. *Tetrahedron*, 2014, 70: 6120–6126; (d) Zhao Q, Tognetti V, Joubert L, Besset T, Pannecoucke X, Bouillon JP, Poisson T. *Org Lett*, 2017, 19: 2106–2109; (e) Casotti G, Fusini G, Ferreri M, Pardini LF, Evangelisti C, Angelici G, Carpita A. *Synthesis*, 2020, 52: 1795–1803
- (a) Feng G, Liu B. *Acc Chem Res*, 2018, 51: 1404–1414; (b) Suleymanov AA, Doll M, Ruggi A, Scopelliti R, Fadaei-Tirani F, Severin K. *Angew Chem Int Ed*, 2020, 59: 9957–9961
- (a) Azpiroz R, Di Giuseppe A, Passarelli V, Pérez-Torrente JJ, Oro LA, Castarlenas R. *Organometallics*, 2018, 37: 1695–1707; (b) Yan R, Wang ZX. *Asian J Org Chem*, 2018, 7: 240–247
- Pagire SK, Föll T, Reiser O. *Acc Chem Res*, 2020, 53: 782–791
- Simmons EM, Hartwig JF. *Angew Chem Int Ed*, 2012, 51: 3066–3072
- According to Tolman’s calculation of electronic parameter, the nucleophilicity of our spirocyclic 6-membered ring’s NHC ligand is much higher than the commonly used 5-membered ring’s imidazole-type NHCs, ranking the second of two top NHCs species so far reported. See: Tolman CA. *Chem Rev*, 1977, 77: 313–348